

# Influence of Thermal Cycle on Temperature Dependent Process Parameters Involved in GTA Welded High Carbon Steel Joints

J. Dutta, Narendranath S.

**Abstract**—In this research article a comprehensive investigation has been carried out to determine the effect of thermal cycle on temperature dependent process parameters developed during gas tungsten arc (GTA) welding of high carbon (AISI 1090) steel butt joints. An experiment based thermal analysis has been performed to obtain the thermal history. We have focused on different thermophysical properties such as thermal conductivity, heat transfer coefficient and cooling rate. Angular torch model has been utilized to find out the surface heat flux and its variation along the fusion zone as well as along the longitudinal direction from fusion boundary. After welding and formation of weld pool, heat transfer coefficient varies rapidly in the vicinity of molten weld bead and heat affected zone. To evaluate the heat transfer coefficient near the fusion line and near the rear end of the plate (low temperature region), established correlation has been implemented and has been compared with empirical correlation which is noted as coupled convective and radiation heat transfer coefficient. Change in thermal conductivity has been visualized by analytical model of moving point heat source. Rate of cooling has been estimated by using 2-dimensional mathematical expression of cooling rate and it has shown good agreement with experimental temperature cycle. Thermophysical properties have been varied randomly within 0 -10s time span.

**Keywords**—Thermal history, Gas tungsten arc welding, Butt joint, High carbon steel.

## I. INTRODUCTION

**G**AS tungsten arc welding (GTA) has been widely used to join ferrous metals (carbon steel of large thickness and thin sections of stainless steel) and non-ferrous metals (aluminum, copper and magnesium alloys).

Rectangular butt joint preparation is one of the most common type of weld joint with a variety of engineering applications such as oil and gas industries, nuclear powerplants, shipbuilding and naval architecture industries and automobile applications.

Basically welding is a process of combined melting and solidification. The development of temperature cycle by movement of GTA torch on the base metal, is produced a drastic change in both thermal and mechanical parameters. Also thermal history has strong influence on hardness of the joint. Thus a clear knowledge about effect of thermal properties based on thermal history is necessary to design a safe and sound structure with higher reliability and longevity. There are so many researchers who have given continuous effort to analyze

thermal properties by applying analytical, mathematical and numerical methodologies to improve as well as to develop a suitable heat source model for implementing in practical field of engineering.

Rosenthal first derived an analytical solution (both 2D and 3D) for solution of temperature distribution in conjunction with several important process parameters namely electrode velocity, thermal diffusivity, radial distance at the velocity field and thermal conductivity [1]. Still now this model is popular for defining thermal cycle. But Rosenthal's model causes serious error based on temperature distribution near the fusion zone (FZ) and heat affected zone (HAZ) due to several predefined assumptions and it has been elaborately pointed out by Myers et al. [2]. Pavelic et al. first proposed a distributed heat flux and have correlated with Gaussian surface heat flux distribution, experimental as well as analytical by defining molten zone, size and shape [3]. Metcalfe and Quigley studied the 'keyhole' distribution of weld pool in gas tungsten arc welding and described the phenomena in relation with electron thermal energy, heat loss due to convection and radiation and gas flow from the GTA nozzle along with anodic heat transfer [4]. To define the heat source and its influence in thermal properties, Goldak et al. established a finite element model based on numerical approach for surface heat source [5]. Tsai and Eagar first successfully implemented non-dimensional variables for determination of temperature distribution in arc welding [6]. Kumar Et al. suggested a new mathematical model based on finite difference method which enables us to visualize the characteristics of heat affected zone (HAZ) by considering several thermophysical properties [7]. Little and Kamtekar analyzed the effect of thermal properties welding efficiency and velocity of moving point heat source during transient temperature developed in arc welding [8]. An excellent studies were carried out by Komanduri and Hou, in his research article 1<sup>st</sup> part consists of finite element method (FEM) based thermal analysis of arc welding of mild steel while 2<sup>nd</sup> part contains of variation of several thermophysical properties as well as their effect on welding process parameters [9], [10]. Zhu and Chao developed FEM code for welding simulation of temperature dependent material properties with detailed non-linear thermomechanical analysis [11]. Poorhaydari K. et al. estimated the peak temperature and cooling rate by implementing temperature distribution correlation on the basis of plate thickness and validated with experimental results [12]. By application of unified mathematical model to define the interaction between GTA welding arc and weld pool has been

Jaideep Dutta and Narendranath S. are with Mechanical Engineering Department of National Institute of Technology Karnataka, Surathkal, India. (e-mail: duttajd1212@gmail.com, snnath88@yahoo.co.in)

portrayed by Lu et al. [13]. Mousavi and Miresmaeili demonstrated experimental and numerical analysis of residual stress distributions in TIG welding of 304L steel in conjunction with the influence of heat capacity, thermal conductivity, elastic modulus, yield stress and flow stress and produced valuable correlation with non-uniform plastic and thermal strains [14]. Zhi et al. explored experimental and numerical analysis of development of temperature cycle by assuming different forms of heat source [15]. Del Coz Diaz investigated comparative analysis of TIG welding distortions of austenitic and duplex stainless steel by incorporating thermograph image analyzer of TIG torch at different positions of weld pool and simulation based work carried out by predicting volumetric heat flux distribution functions [16]. Traidia and Roger introduced a coupling between welding arc and weld pool dynamics by implementing a finite element model and comparisons has been established by using infra-Red camera along with the application of an image processing algorithm [17]. Lee and Chen has developed 3-D finite element models of temperature field induced an alloy 690 butt weld fabricated by GTA welding to investigate sensitization tendencies [18]. By using element free Galerkin method Das et al. reported heat transfer analysis of GTA welding [19]. Pathak et al. proposed a new technique based on coupled convection-radiation heat transfer for calculating rate of heat transfer influenced by temperature cycle from the weld joint during multipass arc welding [20]. Tong et al. established a time-dependent welding heat source model which contains parabolic heat flux distribution at background times and reliability of parabolic model has been validated by conducting experiment as well as with Gaussian heat source model [21]. Dal, Masson and Carin has carried out estimation of time evolution of the weld fusion boundary in spot GTA welding process on a 316L steel disk by implementing iterative regularization method [22]. Ravisankar et al. evaluated temperature distribution with the help of numerical modeling for GTAW circumferential butt joint of AISI 304 stainless steel in connection with the residual stress for different welding velocity [23]. Encouraged by the literature surveys summarized above, present work has been carried out to determine the effect of temperature cycle on temperature dependent properties such as thermal conductivity, cooling rate and heat transfer coefficient. In this work we have incorporate angular torch surface heat flux for analyzing heat flux distribution along the melting region as well as along the longitudinal direction from the weld pool. To visualize the change in cooling rate, contour curves has been portrayed along with temperature history.

## II. MATHEMATICAL MODELS AND THEORETICAL STUDY

In modeling of GTA welding, it is assumed that electric arc has formed moving point heat source depending upon an angular heat source within the weldment.

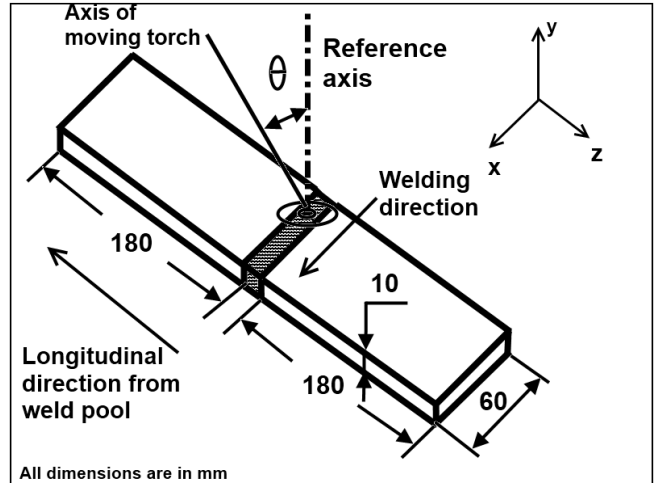


Fig. 1 Schematic diagram of angular moving point heat source

The surface heat model of the arc can be given by [24]:

$$q_{\text{arc}}(x, y, z, t) = \eta_a \cdot \frac{P_{\text{arc}} \cdot \cos \theta}{\pi R_a^2} \exp\left[-\frac{(z - z_0)^2 + (x - vt)^2 \cos^2 \theta}{2R_a^2}\right] \quad (1)$$

where  $\eta_a$  is efficiency of arc energy absorption into the material,  $\theta$  is the inclined angle of the GTA arc torch with reference to vertical axis,  $R_a$  is the effective radius of the arc column and  $v$  is velocity of moving point heat source. To investigate variation of thermal conductivity which has a rapid influence on thermal history developed in GTA welding, Carslaw-Jaeger's analytical model of moving point heat source has been implemented in present analysis and temperature rise can be mathematically expressed as [25]:

$$\Delta T = \frac{Q_{\text{pt}}}{4\pi kR} \exp\left[-\frac{v}{2\alpha}(x + R)\right] \quad (2)$$

where,  $Q_{\text{pt}}(w)$  is source capacity of moving GTA torch ( $Q_{\text{pt}} = \eta VI$ ),  $R$  is radial distance from the weld pool considering weld pool as reference axis ( $R = \sqrt{x^2 + y^2 + z^2}$ ) for specifying space coordinate from weld bead (refer Fig. 1).

For estimating variation of heat transfer coefficient, empirical correlation at low and high temperature has been considered and can be expressed as [14]:

$$h = 0.0668T \text{ (w/m}^2 \text{ }^\circ\text{C) for } 0 < T < 500 \text{ }^\circ\text{C} \quad (3)$$

$$h = 0.231T - 82.1 \text{ (w/m}^2 \text{ }^\circ\text{C) for } T > 500 \text{ }^\circ\text{C} \quad (4)$$

The two kind convective heat transfer coefficient have been used in this article. The first heat transfer coefficient (mentioned in (3)) denotes a combined convection due to airflow and radiation. The second heat transfer coefficient (mentioned in (4)) depicts a compulsive convection created due to rapid flow of inert gas from GTA torch. For validation of (3) and (4), Vinokurov's empirical model of combined convection-radiation heat transfer coefficient has been utilized and it can be expressed as [26]:

$$h_{\text{vin}} = 2.41 \times 10^{-3} \epsilon T^{1.61} \quad (5)$$

To evaluate the rate of cooling along the longitudinal direction from the weld bead, Adam's cooling rate solution for 2-D heat flow has been considered and it can be written as [27]:

$$\frac{dT}{dt} = 2\pi k \rho C_p \left(\frac{d}{H_{\text{net}}}\right)^2 (T_p - T_0)^3 \quad (6)$$

where  $d$  is plate thickness of 10mm,  $T_p$  is peak temperature ( $^{\circ}\text{C}$ ) and  $T_0$  is ambient temperature ( $35^{\circ}\text{C}$ ). The thermophysical properties have been tabulated in Table III.

### III. EXPERIMENTAL WORK

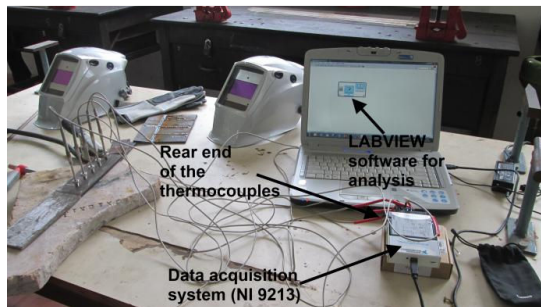


Fig. 2 Representation of experimental setup for thermal cycle investigation

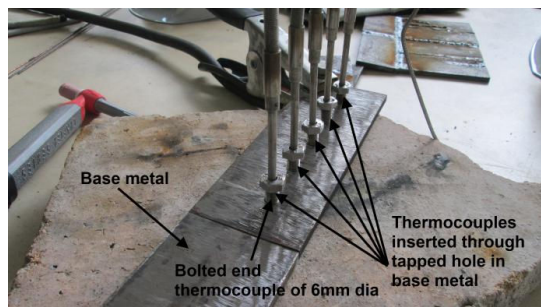


Fig. 3 Mounting of thermocouples in the base metal plate

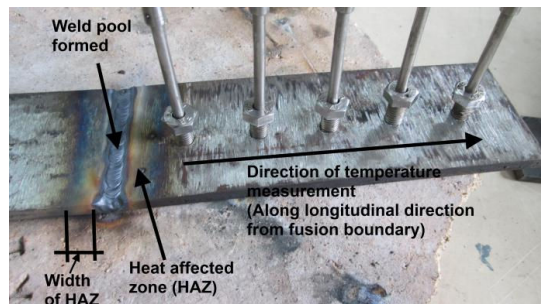


Fig. 4 Direction of temperature cycle and HAZ



Fig. 5 A close view of weld bead and heat affected zone

Experimental set up has been created for determining the temperature cycle developed due to moving GTA torch from starting to till end of the formation of weld bead. To measure the temperature cycle, five K - type thermocouples (6mm round end point with thread and M6 nut attachment) have been inserted on the plate at predefined points keeping 36mm distance between each. The thermocouples have mounted through a 6mm tapped hole on the plate (Fig. 3). Rear end of the thermocouples was connected to NI (National Instruments) 9213 Data Acquisition System (DAQ) for sensing the temperature and the frequency of measurement as well as sensitivity and criteria of time gap for acquiring data has been established through LABVIEW software with the help of programming (Fig. 2). In this measurement 0.1s time gap for each thermocouple has been set to avoid temperature loss and observational errors. The specifications of experimental instruments are tabulated in Table I.

TABLE I  
SPECIFICATIONS OF EXPERIMENTAL APPARATUS

<b>Specimen</b>	Material: AISI 1090 Dimension: 180×60×10
<b>GTA welding System</b>	Welding amperage range: 3-350A, Rated output:250A at 30V, 100% Duty cycle, Maximum open circuit voltage: 75DC
<b>Data Acquisition System (DAQ)</b>	NI 9213 (National Instruments), 16 Channel, 24bit thermocouple, CAT II, Ch. To earth insulation
<b>Filler metal</b>	Copper coated triple de-oxidized mild steel rod
<b>Inert gas used</b>	Argon
<b>Thermocouple</b>	K type

The details of operating variables used for present experiment have been tabulated in Table II.

TABLE II  
EXPERIMENTAL PROCESS PARAMETERS OF CURRENT INVESTIGATION

<b>Input current I (A)</b>	150
<b>Input voltage V (v)</b>	12.8
<b>Time of completing single pass t (s)</b>	70
<b>Electrode speed v (mm/s)</b>	0.857
<b>Heat input <math>P_{\text{arc}}</math> (w)</b>	1632
<b>Arc Heat transfer efficiency <math>\eta_a</math>(%)</b>	85
<b>Radius of GTAW flux <math>R_a</math> (mm)</b>	3
<b>Surface area A (mm<sup>2</sup>)</b>	10800
<b>Heat transfer coefficient <math>h_c</math> (w/m<sup>2</sup>-K)</b>	10
<b>Stefan Boltzmann constant <math>\sigma</math> (J/m<sup>2</sup>-K<sup>4</sup>)</b>	$5.67 \times 10^{-8}$
<b>Emissivity <math>\epsilon</math></b>	0.8

TABLE III  
 THERMOPHYSICAL PROPERTIES OF AISI 1090 [27], [28]

Density $\rho$ (kg/m <sup>3</sup> )	7790
Specific heat $C_p$ (J/kg-°C)	0.465
Thermal conductivity $K$ (w/m-°C)	49.8
Thermal diffusivity $\alpha$ (m <sup>2</sup> /s)	13.74

IV. RESULTS AND DISCUSSION

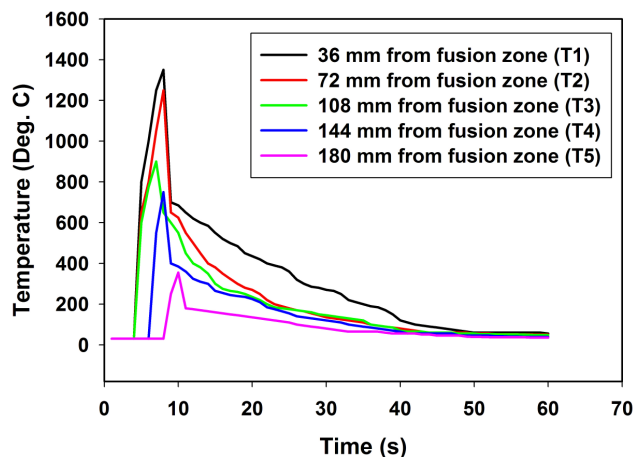


Fig. 6 Experimental temperature history at different points along longitudinal direction from weld pool

Fig. 6 portrays the experimental temperature distribution measured from the data acquired by the thermocouples during movement of moving GTA torch. At  $z = 36\text{mm}$  and  $z = 72\text{mm}$  the maximum temperature peak has been observed, nearer the weld pool. It can be clearly pointed out from Fig. 6 that the heating cycle is very rapid while cooling cycle is very slow and gradual. At  $z = 108\text{mm}$  to  $z = 144\text{mm}$ , temperature peaks went decreasing due to rapid heat loss due to convection and radiation.

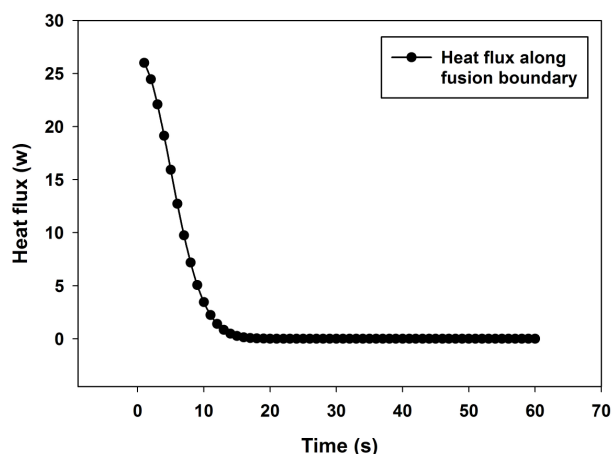


Fig. 7 Heat flux distribution based on angular torch model along weld center line

Near weld bead, influence of radiation is dominant due to continuous flow of argon gas and the effect of coupled convection and radiation. Temperature distribution along

longitudinal direction from weld pool as shown in Fig. 6 has shown well justification with the results shown in [22].

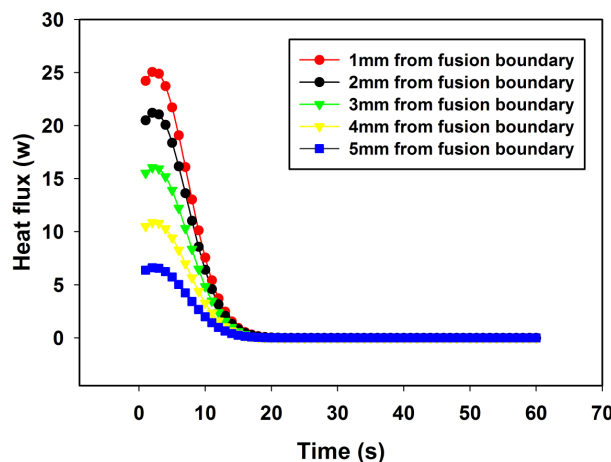


Fig. 8 Heat flux distribution based on angular torch model along longitudinal direction from fusion boundary

In current analysis, angular arc torch model of surface heat flux has been utilized as referred in (1) to investigate heat flux distribution during the formation of weld bead. Fig. 7 describes heat flux distribution along the fusion boundary by maintaining a fixed arc angle of  $45^\circ$ . The effective arc radius has been assumed as 3mm based on literature survey [24]. Theoretically this analysis has been carried out by implementing time simultaneous  $t = 1\text{s}$  to  $t = 60\text{s}$ . This heat flux distribution has been justified by the experimental temperature distribution as described in Fig. 6. Due to generation of arc by pressurized flow of argon gas with non-consumable tungsten electrode, the initial heat flux is very high (0 - 10s) and it is gradually decreasing nature as it moves along the root gap maintained between two plates. In present analysis it has seen that in a time period of 1min and after 23s change in heat flux is almost negligible. Fig. 8 has denoted the variation of heat flux based on angular torch model along the longitudinal direction (refer Fig. 1) from the weld pool. It can be noted that heat flux distribution as mentioned in Fig. 8, is decreasing similar to the thermal cycle provided in Figs. 6 and 7. Heat flux at different positions ( $x = 1\text{mm}, 2\text{mm}, 3\text{mm}$ ) has been investigated for a time period of 60s with constant welding velocity. Compared to change in heat flux along weld pool (refer Fig. 7), after 25s the change in heat flux along longitudinal direction has been found negligible. Figs. 7 and 8 in present paper have fully agreed with the results produced in [13], who discussed the change is anodic heat flux with radial distance along with predefined time span.

Fig. 9 depicts the analysis of temperature rise along the longitudinal direction from weld center line based on theoretical standard values of thermal conductivity at different temperatures [28] from (2). The thermophysical properties near the heat affected zone (HAZ) vary in random manner. In Fig. 9, 0 - 5mm distance specifies the nearest region of melting zone and it can clearly be mentioned that highest thermal conductivity (at lower temperature,  $20^\circ\text{C}$ ) reaches lowest peak temperature and lowest thermal conductivity (at  $600^\circ\text{C}$ ) reaches

highest peak temperature. This result is validated from the point of view of heat transfer as thermal conductivity of metals decreases with the increase in temperature rise [25].

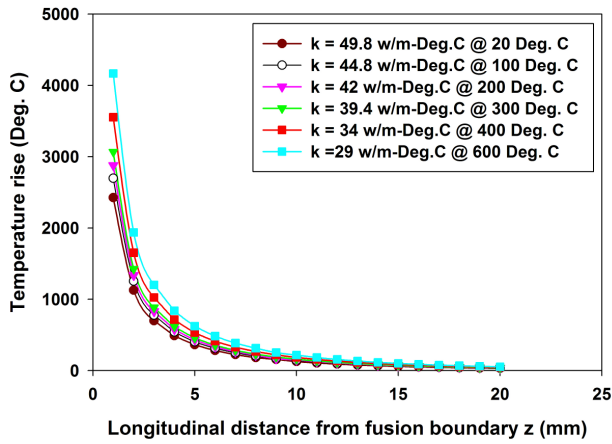


Fig. 9 Variation of temperature rise along longitudinal direction from the weld pool for different thermal conductivity considered different reference temperatures

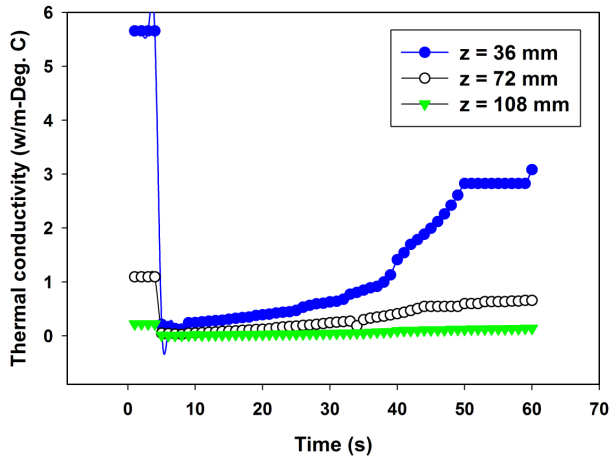


Fig. 10 Variation of thermal conductivity in 60s time span at predefined locations along longitudinal direction from fusion boundary

By incorporating experimental temperature distribution (as shown in Fig. 6) in (2), in a specified time span of 60s, change in thermal conductivity has been studied. Fig. 10 indicates that initially thermal conductivity is linear and due to rapid increase in heating cycle (refer Fig. 6), thermal conductivity suddenly drops in a high rate and very gradually increases with the slow cooling rate along the longitudinal direction from the weld pool. At  $z = 36\text{mm}$  and  $72\text{mm}$ , thermal conductivity has been varied and other locations from the weld pool shows negligible change. The results as depicted in Figs. 9 and 10 can be easily validated by the analysis carried out in [9], [10].

Fig. 11 denotes the variation of heat transfer coefficient of first and second kind as referred in (3) and (4) with the change in time span. From the experimental temperature cycle developed along the longitudinal direction (Fig. 6), heat

transfer coefficient also varies rapidly near the fusion zone and gradually decreases towards the rear end of the butt joint. Equation (4) mentioned the heat transfer coefficient at higher temperatures where convection film on the metal surface produced due to high rate of flow of argon gas and radiation heat transfer due to generation of arc by movement of GTA torch whereas at lower temperatures, heat transfer correlation as mentioned in (3), the effect of convection is dominant than radiation due to heat transfer to atmosphere. The universal coupled heat transfer coefficient i.e. Vinokurov's heat transfer coefficient as expressed in (5), has been implemented for validation. Fig. 11 is clearly indicating the heat transfer coefficient of first and second kind matches with the Vinokurov's empirical correlation for same temperature cycle.

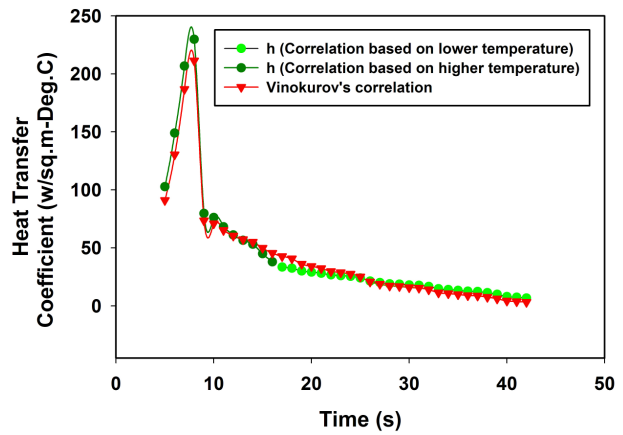


Fig. 11 Change in heat transfer coefficient of first and second kind with Vinokurov's correlation

Cooling rate prediction is one of most important subject as the strength of the joint is dependent on it and it is the deciding factor for any weld joints for structural application. From the Adam's cooling rate (refer (6)) is applicable for estimation of cooling along the longitudinal direction from the weld pool. By application of experimental temperatures keeping other thermophysical properties (refer Table III) as constant, rate of cooling has been analyzed in three different locations from fusion line ( $z = 36\text{mm}$ ,  $72\text{mm}$  and  $108\text{mm}$ ) as depicted in Fig. 12. The higher temperature zone indicates the melting region. The width of HAZ zone is higher for  $z = 36\text{mm}$  due to nearest domain of liquid-solid interface. Also temperature of HAZ at  $z = 36\text{mm}$  is high ( $\approx 1200^\circ\text{C}$ ) compared to  $z = 72\text{mm}$  and  $z = 108\text{mm}$  due to random heat loss and propagation of solidification wavefront. Also it can be pointed out from Fig. 12 that cooling rate is slow at  $z = 36\text{mm}$  and  $z = 72\text{mm}$  whereas it is relatively higher at  $z = 108\text{mm}$ .

Thus gradual cooling rate is similar to the temperature cycle as denoted in Fig. 6. The information containing in Fig. 12 shows good agreement with the research article as denoted in [20], [21].

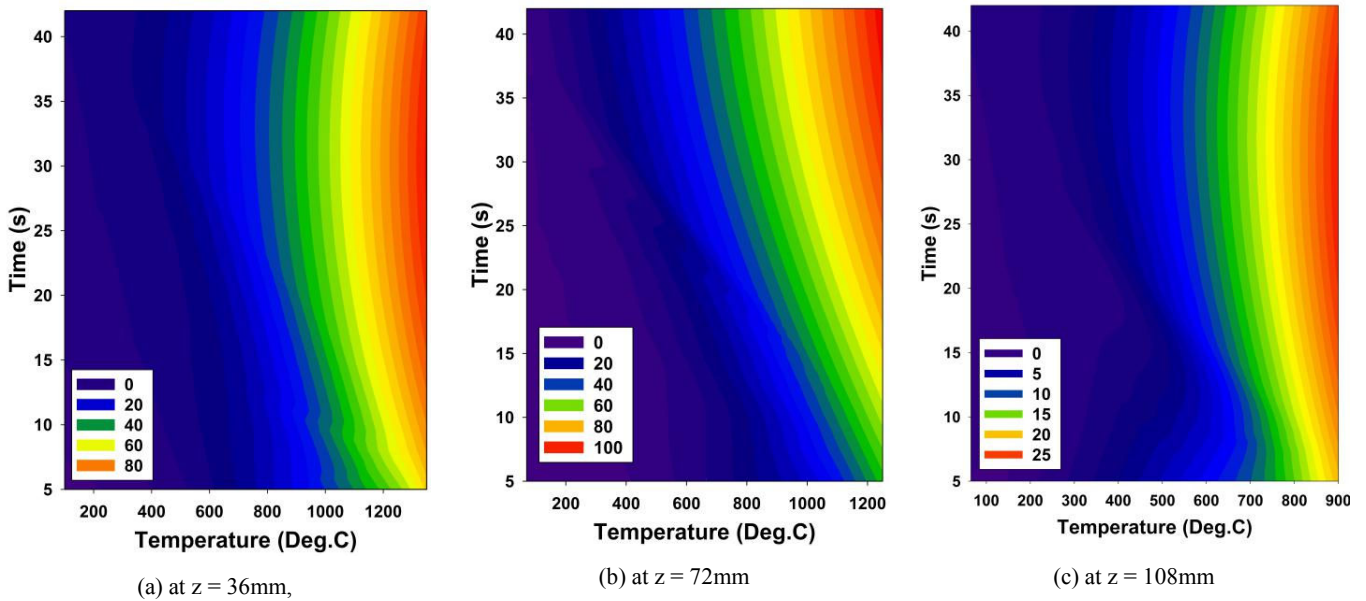


Fig. 12 Propagation of cooling rate wavefront from fusion line to longitudinal direction

## VI. CONCLUSION

From the current investigation the following statements can be considered as concluding remarks:

- Experimental temperature history consists of very high heating cycle and a slow gradual cooling cycle. Only 0 - 10s time is required to produce peak temperature followed by cooling with solidification phenomena.
- Angular torch heat flux model gives justification of experimental temperature cycle. It can be compared with Goldak's double ellipsoidal model and Gaussian distribution. With the change in angle of GTA torch maintained during the time of welding is important parameter to be considered to provide smooth and sound weld bead.
- Thermal conductivity is an important thermophysical property to be considered in thermal analysis. It is only variant in the HAZ region. It defines the acceptability of Carslaw-Jaeger's mathematical model of moving point heat source at higher temperature.
- Heat transfer coefficient of first and second order is important parameters as it exactly matches with the Vinokurov's empirical correlation and it can be major parameter during transient thermal analysis of weld joints.
- Cooling rate along the longitudinal direction from the weld pool has followed the experimental temperature profile. It is maximum at  $z = 72\text{mm}$  as estimated from the weld pool at  $z = 108\text{mm}$  temperature falls gradually and slow cooling rate has been observed compared with two other locations.

## ACKNOWLEDGMENT

We would like to express our gratitude to the Department of Mechanical and Manufacturing Engineering of Manipal Institute of Technology (MIT Mangalore, India) for the support to carry out the GTA welding facility in their

laboratory. Authors are thankful to Prof. Nagaraja, Superintendent of Mechanical workshop for his continuous help and encouragement. We are thankful to technical faculty members of welding laboratory for sharing their valuable knowledge to complete the experiment.

## REFERENCES

- Rosenthal D., "The theory of moving sources of heat and its applications to metal treatments", Trans. ASME, Vol. 68, 1946, pp. 849-865.
- Myers P. O. Et al., "Fundamentals of heat flow in welding", Welding Research Council Bulletin, 1967, no. 123.
- Pavelic V. Et al., "Experimental and computed temperatures histories in gas tungsten arc welding of thin plates, Welding Journal Research Supplement", 1969, Vol. 48, pp. 2952-305s.
- Metcalfé J.C. and M. B. C. Quigley; "Heat Transfer in Plasma Arc Welding", Welding Research Supplement, AWS, 1975, vol. 3, pp. 99 - 104.
- Goldak J. Et al.: "A finite element model for welding heat sources", Metallurgical Transactions B., 1984, vol. 15B, pp. 299 - 305.
- Tsai N. S. and Eagar T. W.; "Changes of weld pool shape by variation in the distribution of heat source in arc welding", Modeling of Casting and Welding Processes II, 1984, AMIE New York, 317.
- Kumar B. V. Et al., "Welding of Thin Plates: A new model for thermal analysis", Journal of Materials Science (Chapman and Hall), 1992, vol. 27, pp. 203 - 209.
- Little G. H. and Kamtekar A. G., "The effect of thermal properties and weld efficiency on transient temperatures during welding", Computers and Structures, 1998, vol. 68, pp. 157 - 165.
- Komanduri R. and Hou Z. B., "Thermal analysis of arc welding process: part I. General solutions", Metallurgical and Materials Transactions B, 2000, Vol. 31B, pp. 1353 - 1370.
- Komanduri R. and Hou Z. B., "Thermal analysis of arc welding process: part II. Effect of thermophysical properties with temperature", Metallurgical and Materials Transactions B, 2001, Vol. 33B, pp. 483 - 499.
- Zhu X. K. and Chao Y. J., "Effect of temperature dependent material properties on welding simulation", Computers and Structures, 2002, vol. 80, pp. 967 - 976.
- Poorhaydari K. Et al., "Estimation of cooling rate in the welding of plates with intermediate thickness", Welding Journal, 2005, pp. 149s - 155s.
- Lu Fenggui Et al., "Numerical simulation on interaction between TIG welding arc and weld pool", Computational Materials Science, 2006, vil. 35, pp. 458 - 465.

- [14] Mousavi Akbari S. A. A. and Miresmaeili R., "Experimental and numerical analyses of residual stress distributions in TIG welding process for 304L stainless steel", *Journal of Material Processing Technology*, 2008, vol. 208, pp. 383 - 394.
- [15] Zeng Zhi Et al., "Numerical and experimental investigation on temperature distribution of the discontinuous welding", *Computational Materials Science*, 2009, vol. 44, pp. 153 - 1162.
- [16] Del Coz Diaz J. J. Et al., "Comparative analysis of TIG welding distortions between austenitic and duplex stainless steels by FEM", *Applied Thermal Engineering*, 2010, vol. 30, pp. 2448 - 2459.
- [17] Traidia A. and Roger E., "Numerical and experimental study of arc and weld pool behaviour for pulsed current GTA welding", *International Journal of Heat and Mass Transfer*, 2011, vol. 54, pp. 2163 - 2179.
- [18] Lee Hwa Teng and Chen Chun Te, "Predicting effect of temperature field on sensitization of alloy 690 weldments", *Materials Transactions, The Japan Institute of Metals*, vol. 52 (9), pp. 1824 - 1831.
- [19] Das R. Et al., "Welding heat transfer analysis using element free galerkin method", *Advanced Materials Research*, 2012, vol. 410, pp. 298 - 301.
- [20] Pathak C. S. Et al., "Analysis of thermal cycle during multipass arc welding", *Welding Journal*, 2012, vol. 91, pp. 149s - 154s.
- [21] Tong Zhang Et al., "A dynamic welding heat source model in pulsed current gas tungsten arc welding", *Journal of Material Processing Technology*, 2013, vol. 213, pp. 2329 - 2338.
- [22] Dal Morgan, Masson Philippe Le and Carin Muriel, "A model comparison to predict heat transfer during spot GTA welding", *International Journal of Thermal Sciences*, 2014, vol. 75, pp. 54 - 64.
- [23] Ravisankar A. Et al., "Influence of welding speed and power on residual stress during gas tungsten arc welding of thin sections with constant heat input: A study using numerical simulation and experimental validation", *Journal of Manufacturing Processes*, 2014, vol. 16, pp. 200 - 211.
- [24] Kong Fanrong and Kovacevic Radovan, "3D finite element modeling of the thermally induced residual stress in the hybrid laser/arc welding of lap joint", *Journal of Material Processing Technology*, 2010, vol. 210, pp. 941 - 950.
- [25] Carslaw H. S. and Jaeger J. S., "Conduction of Heat in Solids", Oxford University Press, 2<sup>nd</sup> ed., 1959, Oxford, United kingdom.
- [26] Desai R. S. and Bag S., "Influence of displacement constraints in thermomechanical analysis of laser micro-spot welding process", *Journal of Manufacturing Process*, 2014, vol. 16, pp. 164 - 175.
- [27] Kou Sindo, "Welding Metallurgy", Willey-Interscience, A John Willey and Sons inc. Publication, 2<sup>nd</sup> ed., 2003, 111 River street, Hoboken, New Jersey 07030.
- [28] ASM Handbook, "Welding, Brazing and Soldering", ASM International, Vol. 6, 1993.